

AD-A085 998

CARNEGIE-MELLON UNIV PITTSBURGH PA DEPT OF METALLURG--ETC F/G 11/6
STATUS REPORT FOR PERIOD 1 NOVEMBER 1970 TO 30 APRIL 1980. (U)
APR 80

N00014-75-C-0265

NL

UNCLASSIFIED

1 of 1



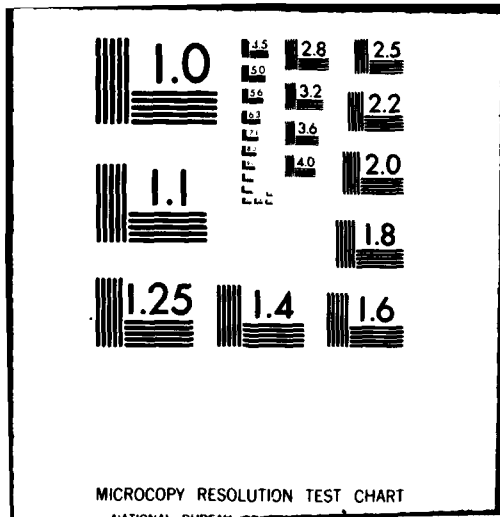
END

DATE

FILED

8-80

DTIC



Carnegie Mellon Univ
Pittsburgh, PA
Dept of Metallurgy and
Materials Science

LEVEL

(1)

036-000
TiC
JUN 25 1980

(6) Status Report for Period 1 November 70 to 30 April 1980.

Contract N00014-75-C-0265

(11) 30 Apr 80

(15)

(12) 10

ADA 085998

→ This report summarizes our progress on two current areas of investigation:

The use of strengthening particles as innocuous hydrogen traps and hydrogen-induced twin formation in iron-titanium alloys. ←

Trapping by TiC Particles

Studies have continued on the resistance of an HSLA steel to hydrogen embrittlement. Specifically, we have correlated hydrogen diffusivity data and microstructural analysis with the observed mechanical behavior of the alloy containing internal hydrogen.

Figure 1 shows the effect of microstructure on subsequent hydrogen transport in the alloy with a composition of 1.37% Mn, 0.22% Ti, 0.064% C and 0.26% Si. All specimens were solution annealed followed by quenching and aging at temperatures from 600°C to 900°C. Diffusion coefficients measured from the first polarization reflect the influence of the total trapping population, including dislocation, grain boundaries, substitutional atoms, voids and second phase particles (TiC). Second transient diffusivities are affected only by the reversible trap density, as the irreversible traps remain filled. The largest difference is observed for the 600°C age, reflecting the optimum combination, for this alloy, of the strength and number of irreversible traps. Since the only considerable change in the microstructure for these heat treatments, compared to the as-quenched condition, is the nucleation and growth of TiC particles, it is reasonable to believe that they are responsible for the irreversible trapping. At temperatures above 600°C, the yield strength decreases and the microstructure

DDC FILE COPY

This document has been approved for public release and sale; its distribution is unlimited.

404 459

80 6 13 018

[Handwritten signature]

changes from an acicular to a recrystallized ferrite. These changes and the expected coarsening of the TiC particles are reflected in diminution of the extent of irreversible trapping.

These data have been quantified in Figure 2 which shows particle size and density counts as determined from transmission electron micrographs. As reported earlier, it is known that these carbides are coherent with the matrix up to a size of 30Å and become fully incoherent at sizes of 200Å. In regard to the relative trapping densities in the 600, 700 and 900°C aged treatments, this implies both that the surface-to-volume ratio of these carbides is the important parameter for determining total trapping density, and that fine semi-coherent particles provide a good irreversible trapping structure.

Data reported previously by us have shown that the 600°C treatment provides the best resistance to hydrogen embrittlement, in agreement with our assessment of the beneficial role of a fine distribution of semi-coherent particles. This positive effect disappears with increased hydrogen content indicating that these are saturable traps. After supersaturating the matrix with a 24 hr charge, the fracture mode changes from dimpled rupture to a predominantly intergranular mode with localized cleavage "bursts" on the facets. In these quenched and aged treatments, grain boundary precipitation of alloy carbides is known to occur. It is not yet known, however, if this intergranular failure mode is associated with grain boundary precipitates or with transport of hydrogen to these sites by dislocation during the test.

Future Work

We plan sustained load cracking tests on this material in order to observe how microstructural manipulation affects hydrogen embrittlement susceptibility

during sustained load cracking.

We will be extending these studies to a set of alloys thought to have more ideal compositions for irreversible trap control. These are being provided through the courtesy of Bethlehem Steel Corporation and will have the following compositions:

Fe - 0.05w/oC-0.30w/oTi

Fe - 0.10w/oC-0.15w/oTi

Fe - 0.10w/oC-0.40w/oTi-1.0w/oMn

Students of Professor H. I. Aaronson will be examining the phase transformation characteristics of the first two heats and we will compare the hydrogen permeability and mechanical properties in order to further deduce the role of Mn and TiC on trapping and strength.

Twin Formation in Fe-Ti

This work shows promise of providing needed information on how hydrogen affects the fundamental bonding between iron atoms.

Three different titanium and carbon content iron alloys have been fully studied. The compositions of them are shown in Figure 3. The TiC particles distributions is also shown in Figure 3. As we can see, alloy B has the largest amount of TiC particles, which are strong, irreversible hydrogen traps.

As reported previously, ambient cathodic charging of hydrogen into these alloys can induce both additional dislocations and twin formation, with the formation of twins strongly dependent on alloy content. In fact, only alloy B exhibits twinning formation. The twins found in alloy B have been classified as compound twins with a {112} twinning plane and a $\langle 111 \rangle$ twinning axis. Figure 4 shows a series of pictures of twin formation in alloy B for different charging time. In all cases, twins are found at or near TiC particles with the size of

the twins increasing as the amount of internal hydrogen increases. The largest twin, found in 30 minute charged specimens, is almost twenty times larger than the smallest twin, occasionally found even in uncharged specimens. This suggests that twinning growth can be achieved by the interaction between TiC particles and hydrogen.

Future Work

Because twinning in bcc iron alloys has only previously been found during low temperature or high strain rate deformation, it is necessary to determine why twins are present in uncharged specimens and to elucidate how the presence of hydrogen increases both their number and size. In a future experiment, we will solutionize alloy B and then use different cooling rate to control size and density distribution of TiC particles, to determine the dependence of twinning formation on TiC particle distributions. In a second experiment, we will charge hydrogen into the specimen when it is in its stable austenite phase structure to see if the twins are transformation related.

Accession For	
NTIS GRA&I	
DOC TAB	
Unannounced	
Justification <i>for</i>	
<i>50 samples</i>	
By _____	
Distribution/	
Availability Codes	
Dist	Avail and/or special
A	

ONR Related Publications 1979-1980

1. "Effect of Structural Inhomogeneities on the Hydrogen Embrittlement of Steel", Trans. Japan Institute of Metals 21, 1980, p 429 (with A. W. Thompson).
2. "Effect of Hydrogen on the Slip Behavior of Nickel", Acta Met 28, 1980, p 701 (with W. A. McInteer and A. W. Thompson).
3. "Effect of Hydrogen on Ductile Fracture in Spheroidized Steels", Met. Trans., in press (with R. Garber and A. W. Thompson).
4. "Effect of Microstructure on Stress Corrosion Cracking of HY130 Steel", Met. Trans., in press (with C. Chen and A. W. Thompson).
5. "Effect of Hydrogen Trapping on Hydrogen Embrittlement", Met. Trans., in press (with G. Pressouyre).

Oral Presentations 1979-1980

- February: Microstructural Effects on Fracture in Plain Carbon Steel
AIME Annual Meeting, Las Vegas, NV
- March: Microstructural Control of Hydrogen Embrittlement
Exxon Research, Linden, NJ
- April: Hydrogen Embrittlement of Steel
Bethlehem Steel (at C-MU)
- June: Microstructural Control of Hydrogen Embrittlement in Low and Medium
Strength Steels
Case Western Reserve University, Cleveland, OH

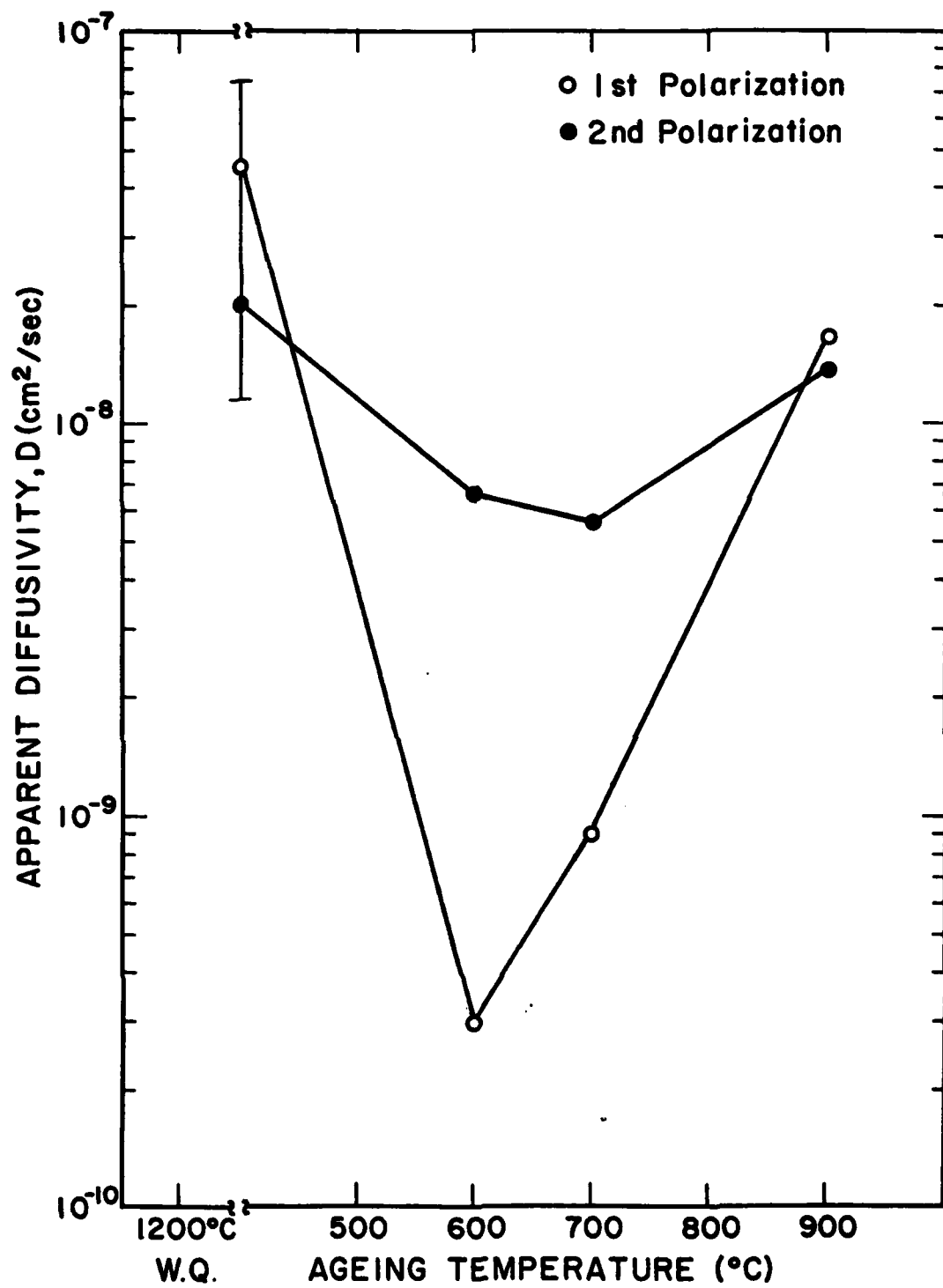


Figure 1. First and Second Hydrogen Permeation Transients.

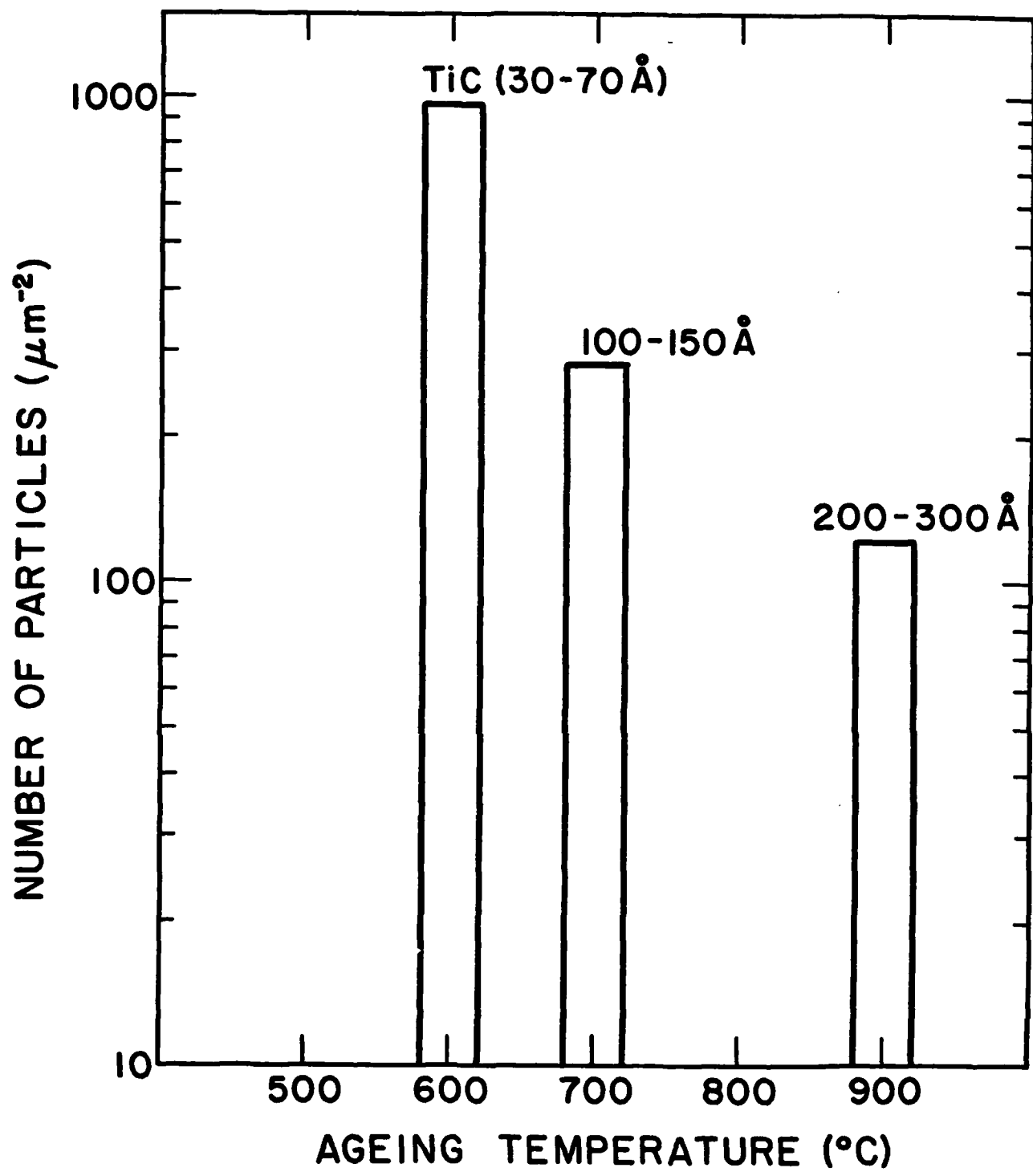


Figure 2. Size and Distribution of TiC Particles.

alloy	Ti wt%	C wt%	N wt%	O wt%
A	0.15	0.005	0.0022	0.0039
B	0.50	0.065	—	—
C	1.38	0.039	—	—

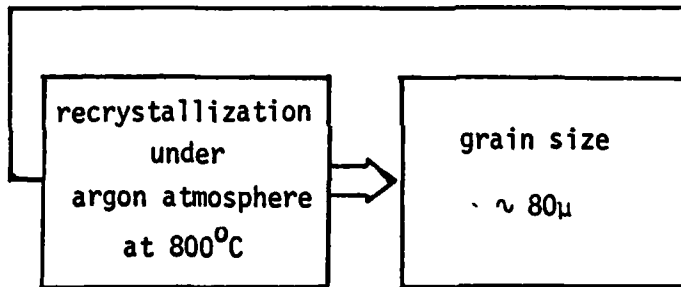
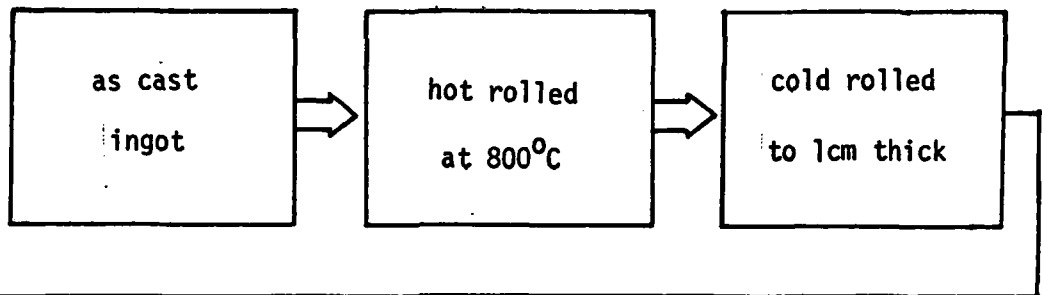
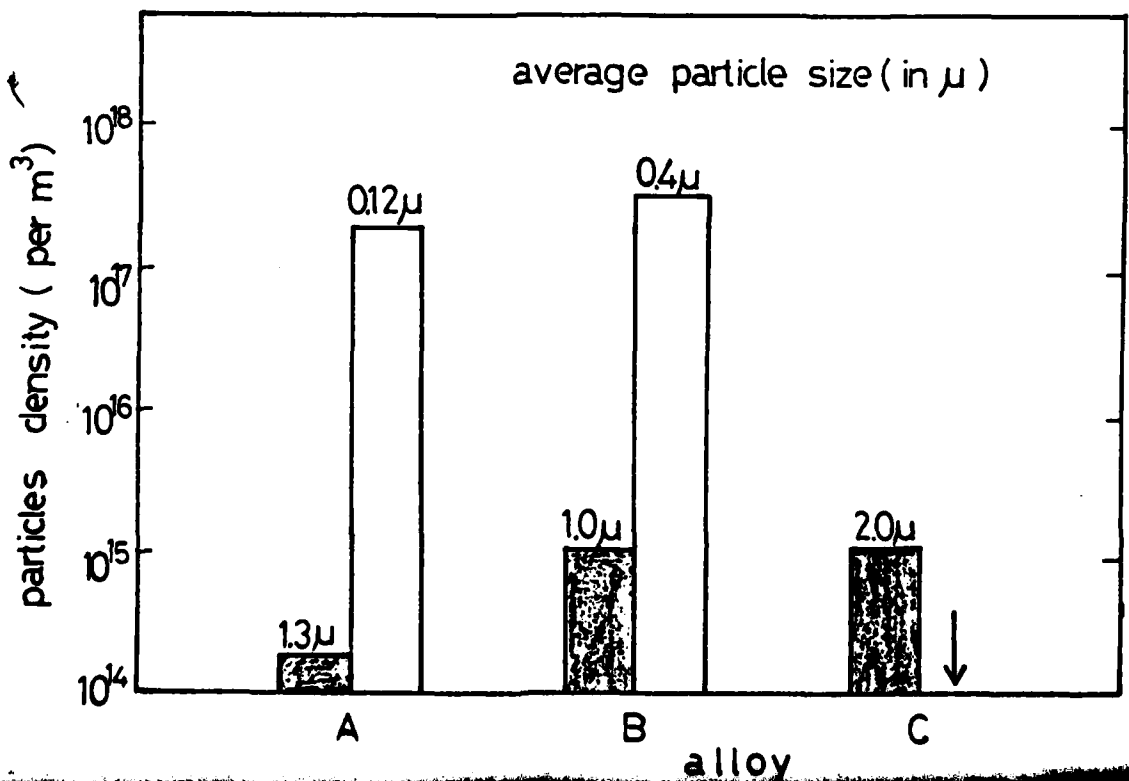


Figure 3. Alloy Compositions and TiC Particle Densities.





A. 2500A

Figure 4a. Bright Field Image of Twins in 15 Min. Charged Alloy B.



Figure 4b. Bright Field Image of Twins in 30 Min. Charged Alloy B.